Int. J. Electrochem. Sci., 14 **(2019)** 919 – 928, doi: 10.20964/2019.01.78

International Journal of
ELECTROCHEMICAL
SCIENCE
www.electrochemsci.org

The Influences of Chloride Anions on Corrosion Electrochemical Characteristics of 904L Stainless Steel in Blast Furnace Gas/Water system

Liang chao Chen[1], *Pei Zhang*[2], *Qing yun Xiong*[3], *Pan Zhao*[3], *Jin ping Xiong*[3,*], *Yong Zhou*[4,**]

[1] College of Mechanical and Electrical Engineering, Beijing University of Chemical Technology, Beijing 100029, China
[2] Guangxi Key Laboratory of Agricultural Resources Chemistry and Biotechnology, College of Chemistry and Food Science, Yulin Normal University, Yulin 537000, China
[3] College of Materials Science and Engineering, Beijing University of Chemical Technology, Beijing 100029, China
[4] Key Laboratory for Green Chemical Process of Ministry of Education, Wuhan Institute of Technology, Wuhan 430205, China
[*] E-mail: xiongjp@mail.buct.edu.cn
[**] E-mail: zhouyong@wit.edu.cn

Received: 2 October 2018 / *Accepted:* 13 November 2018 / *Published:* 30 November 2018

In this work, the influences of chloride anion (Cl^-) concentrations on the corrosion electrochemical characteristics for a super austenitic stainless steel (ASS), 904L ASS, in a simulated environmental solution that was acquired with the introduction of blast furnace gas (BFG) into water were investigated with the methods of electrochemical techniques including potentiodynamic polarization, electrochemical impedance spectroscopy (EIS), current transient and Mott-Schottky plot. From the electrochemical measurement and investigation, the results showed that 904L ASS presented the electrochemical behavior of self-passivation in the BFG/water solutions with different concentrations of Cl^-, and the influences of Cl^- concentrations on the main corrosion electrochemical parameters, including pitting potential (E_{pit}), passivation current density (i_{pass}), repassivation potential (E_{rep}), passive film capacitance (CEP_f), passive film resistance (R_f), flat bond potential (U_{fb}) and donor density (N_D), were very prominent and showed a certain rule. Further, the 904L steel presented the good self-passivation characteristic in the BFG/water solution when the Cl^- concentration was lower than 78.50 g/L. However, when the Cl^- concentration was higher than 78.50 g/L, the self-passivation characteristic of 904L ASS decreased gradually with the increase of Cl^- concentration. Further, the relation between corrosion and passivation characteristics was also discussed in this paper.

Key words: 904L ASS; corrosion and passivation; blast furnace gas; chloride anion; polarization; EIS; Mott-Schottky

1. INTRODUCTION

Due to the perfect corrosion resistance and the good mechanical performance, ASSs are widely used in various industries, such as atomic energy, traffic transportation and chemical production and so on [1-4], which is attributed to the presence of stable and self-healed passive film [5-7]. At present, in order to satisfy the requirements of military and civil fields, the improvement of traditional ASSs and the development of new ASSs are paid more and more attention by materials scientists and engineers [8]. As a new type of ASSs with the high elements of molybdenum(Mo) and nickel (Ni), 904L ASSs have been developing quickly and show the good application in the chemical industries of phosphoric acid and concentrated sulfuric acid, which is attributed to the combination of excellent corrosion resistance and perfect physical property [9].

Recently, investigations on corrosion and protection for 904L ASSs are the following two points: the properties of passive film on the 904L surface and the electrochemical characteristics of 904L ASSs in service environments [10-14], which are attributed to the superiority for 904L SSs on the combined performance and the wide application. Alamr et al [10] compared the properties of passive film involving mechanical strength and corrosion resistance for 904L ASS and 316L ASS with the electrochemical and nanoindentation techniques. The authors reported that the passive film on the surface of 904L steel was denser that that on the surface of 316L steel, resulting in that the former film showed the better load capacity and corrosion resistance than the later film did. Further, it was found that the addition of Gr element in 904L ASS was responsible for the improvement. Meguid et al [11] studied the pitting behavior of 904L steel in chloride-sulphide solutions with electrochemical measurement and microstructural observation and reported that the values of pitting potential (E_{pit}) moved to the negative direction with the rise of temperature and the increased of S^{2-} concentration. Raja et al. [12] studied the effect of N element on the weld cladding and pitting corrosion of 904L steel. The authors reported that the addition of N element to the weld cladding decreased the amount of γ_2 phase and restrained the pitting susceptibility. Michalska et al [13] studied the effect of H element on the corrosion resistance of 904L steel and reported that the hydrogenation could decrease the stability of passive film and increased the corrosion rate of 904L steel. Further, the surface ductility of 904L steel also was reduced. Moayed et al. [14] studied the influences of sulfate anions on the critical pitting temperature (CPT) and the pitting behavior of 904L steel in chloride solutions containing the different concentration of SO_4^{2-}. The authors reported that the value of E_{pit} increased with the increase of SO_4^{2-} concentration when the temperature was higher than the value of CPT. However, the CPT value decreased with the increase of SO_4^{2-} concentration.

Blast furnace gas (BFG) is a universal contaminate gas in industrial production, which is usually introduced into an absorbed water to decrease environmental contamination. Further, stratum water is generally used as the absorbed water due to low cost and convenient source. In our previous work, the influences of Cl^- on corrosion and passivation characteristics of a super austenitic stainless steel (254SMO) have been investigated [15]. At present, the application of 904L ASSs in the industrial circle involving BFG is more and more wide, but it is not clear for the corrosion electrochemical characteristics of 904L steel in the absorbed water containing BFG, especially the influences of Cl^- concentrations in the BFG/water system. In this paper, a mixture of electrolyte including Fe^{2+}, Ca^{2+},

SO_4^{2-}, NO_3^-, PO_4^{3-} and Cl^- is used to simulate the practical component of BFG/water system, and the concentration of chloride anions is changed through the direct addition of sodium chloride (NaCl). The electrochemical measurements of potentiodynamic polarization, electrochemical impedance spectroscopy (EIS), current transient and Mott-Schottky plot are carried out.

2. EXPERIMENTAL

2.1 Material and solution

The tested object was 904L ASS, and the chemical composition (wt%) of 904L steel was as follows: C, 0.015; Cr, 20.770; Ni, 23.500; Mn, 1.550; Si, 0.580; P, 0.028; S, 0.035; Mo, 4.560; N, 0.150; Cu, 1.500; and Fe, balance. Specimens were abraded up to 1000 grit manually with water abrasive papers, then rinsed with de-ionized water and, after that, degreased in acetone.

The electrolyte for electrochemical measurements was a solution with the absorption of BFG by water and the component was as follows: Fe^{2+}, 9.102 g/L; Ca^{2+}, 0.332 g/L; SO_4^{2-}, 4.260 g/L; NO_3^-, 8.161 g/L; PO_4^{3-}, 0.078 g/L; and Cl^-, 78.500 g/L. Further, to investigate the Cl^- influences on corrosion electrochemical characteristics, the concentration of Cl^- was changed through the direct addition of analytical pure grade NaCl. The investigated concentration range of Cl^- in this work was from 20 g/L to 120 g/L.

2.2 Electrochemical measurement

Electrochemical measurements of potentiodynamic polarization and current transient were performed with a CS350 electrochemical instrument (China), and electrochemical measurements of EIS and Mott-Schottky plot were carried out with a Princeton 2273 electrochemical instrument (USA). A typical three electrode system was applied for all the electrochemical tests, which was composed of a saturated calomel electrode (SCE) as reference electrode, a platinum sheet as counter electrode and the 904L specimen as working electrode. Before each electrochemical test, the working electrode was immersed in the tested solution for a certain period of time until the open circuit potential (OCP) to be stable. In the polarization curve test, the potential scanning rate was 0.5 mV/s, and the potential scanning range was from -0.2 V_{OCP} to the potential value when the repassivation potential was obtained. In the EIS test, a perturbation potential of 10 mV amplitude was used in the frequency range from 10^5 Hz to 10^{-2} Hz. In the current transient test, a constant potential of 0.5 V_{SCE} was used on the 904L specimens, and the recording frequency of current density was 5 Hz. In the Mott-Schottky plot test, the potential scanning rate was 5 mV/s, and the potential scanning range was from -0.6 V_{SCE} and 0.6 V_{SCE}.

The electrochemical measurements were performed at 50 ℃, and the temperature was controlled with an electro-thermostatic water bath.

3. RESULTS AND DISCUSSION

3.1 Potentiodynamic polarization

Fig. 1 shows the potentiodynamic polarization curves of the 904L specimens in the BFG/water solutions containing the different Cl^- concentrations. From Fig. 1, in the investigated range of Cl^- concentration, the i_{pass} values for the specimens are approximately 10^{-5} A/cm^2, suggesting that all of the specimens showed the self-passive behavior in the BFG/water system [16]. Besides, the influences of Cl^- concentrations on the values of corrosion potential (E_{corr}), i_{pass}, E_{pit} and E_{rep} are very obvious, as shown in Fig. 1.

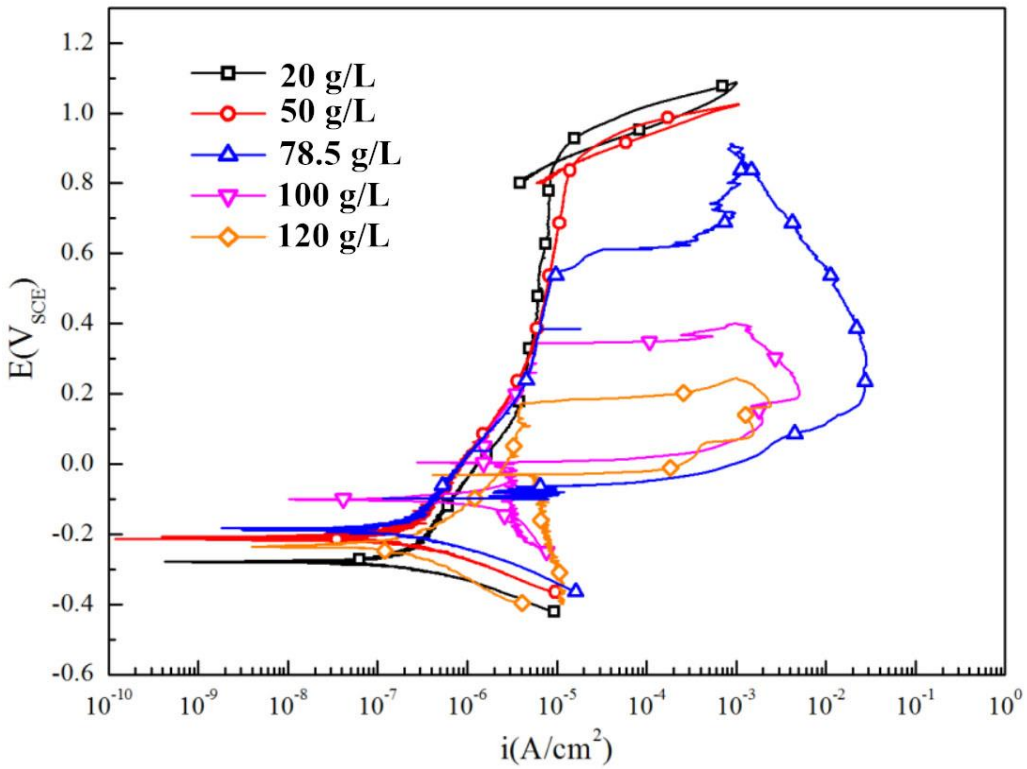

Figure 1. Potentiodynamic polarization curves of 904L specimens in BFG/water solutions containing different Cl^- concentrations.

Table 1 presented the fitted values of i_{pass}, E_{pit}, E_{rep} and (E_{pit} - E_{rep}) from the potentiodynamic polarization curves, as shown in Fig. 1. From Table 1, it is seen obviously that the values of i_{pass} increase and the values of E_{pit} as well as E_{rep} decrease with the increase of Cl^- concentration in the BFG/water solution, which indicates that the self-passive characteristic occurred easier at the low concentration of Cl^- than at the high concentration of Cl^- did. Further, it is worth noting that when the Cl^- concentration was 120 g/L, the range of passivation potential is too short, suggesting no passivation process. Similar results are also reported by Lv et al. [17] and Tian et al. [18].

Table 1. Fitted values of passivation current density (i_{pass}), pitting potential (E_{pit}), repassivation potential (E_{rep}) and potential difference between pitting potential and repassivation potential (E_{pit} - E_{rep}).

$[Cl^-]$ (g/L)	i_{pass} ($\mu A/cm^2$)	E_{pit} (V_{SCE})	E_{rep} (V_{SCE})	(E_{pit} - E_{rep}) (V_{SCE})
20	5.290	1.020	0.864	0.156
50	5.300	0.972	0.825	0.148
78.5	5.670	0.616	-0.063	0.680
100	5.800	0.350	-0.051	0.401
120	--	0.193	-0.039	0.232

However, compared with 254SMO ASS in the same electrolyte [15], it is seen that the self-passive characteristic of 904L steel is worse than that of 254SMO steel. In the investigated concentration range of Cl^- from 20 g/L to 120 g/L, the values of E_{pit} and E_{rep} for the 254SMO steel are approximately 1.0 V_{SCE}, but the corresponding values for the 904L steel is relatively low. Further, from the values of E_{pit} and (E_{pit} - E_{rep}), the pitting susceptibility of 904L steel is also increased with the increase of Cl^- concentration in the BFG/water system. Similar results are also observed in 254SMO ASS in our previous study [15] and reported in other stainless steel by Tang et al. [19], Feng et al. [20] and Huang et al. [21].

3.2 Electrochemical impedance spectroscopy

Fig. 2 shows the EIS of the 904L specimens in the BFG/water solutions containing the different Cl^- concentrations. From Fig. 2a, each Nyquist plot shows a single capacitive loop in the measured range of applied frequency. It was reported that capacitive loops reflected EIS behavior of surface film and double electron layer on the surface of metals and alloys [22]. In the present study, the presence of single capacitive loop is attributed to the surface passive film on 904L ASS. Further, the results shown in Nyquist plots also suggest that for 904L ASS, the process of charge transfer is absent and the passive film on the surface of 904L ASS presents good corrosion resistance and provides great protection for the steel substrate.

On the one hand, from Fig. 2a, the radii of the capacitive loops decrease gradually with the increase of Cl^- concentrations. On the other hand, from Fig. 2b, for the impedance modulus at the low frequency limit of 0.01 Hz, the modulus values also decrease gradually with the increased Cl^- concentrations. The above results of EIS indicate that in the investigated range of Cl^- concentration, the self-passive characteristic of 904L ASS at the low Cl^- concentration is greater than that at the high Cl^- concentration. At the same time, regardless of Cl^- concentrations in the BFG/water solutions, no second capacitive loop is shown in each Nyquist plot, suggesting a stable self-passive condition on the surface of 904L ASS. It can be concluded that 904L ASS would show a great corrosion resistance in the BFG/water system.

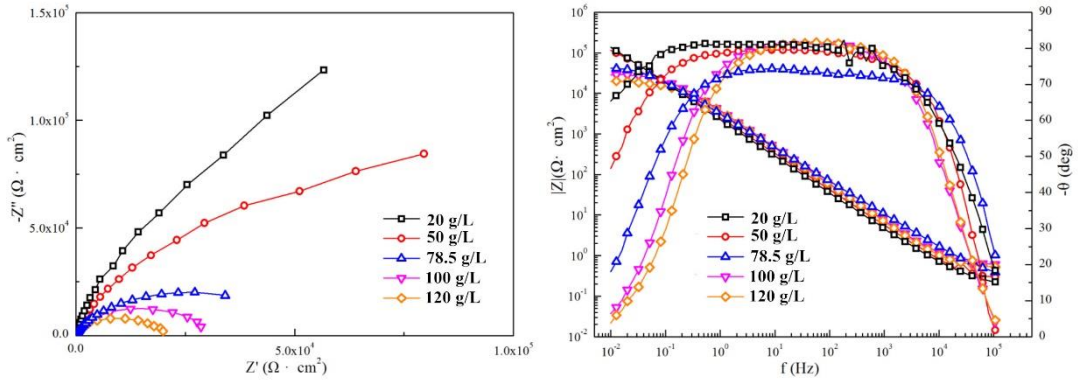

Figure 2. EIS of 904L specimens in BFG/water solutions containing different Cl^- concentrations: (a) Nyquist plots and (b) Bode plots.

Further, in order to clarify the influences of chloride anions on the EIS characteristics of 904L ASS in the BFG/water solutions with the different Cl^- concentrations, the interpretation of equivalent electrical circuit (EEC) was used. According to the EIS results in Fig. 2 and other previous study [23-25], EEC model shown in Fig. 3 is used to interpret the EIS results. In Fig. 3, R_s is the solution resistance, and R_f and CPE_f are the passive film resistance and the passive film capacitance, respectively.

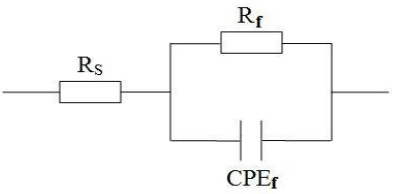

Figure 3. Equivalent electrical circuit (EEC) model.

Table 2 shows the interpreted values of R_f and CPE_f from the results of EIS, as shown in Fig. 2. The value of R_f could reflect the corrosion resistance of surface film for metals and alloys [26]. From Table 2, the R_f values decrease obviously with the increase of Cl^- concentrations in the BFG/water solutions. At the same time, the value of CPE_f could indicate the actual destructive area on the surface of metals and alloys [27]. From Table 2, the values of CPE_f for the 904L steel at the low Cl^- concentration are less than those at the high Cl^- concentration. The values of R_f and CPE_f suggest that for the passive film on the surface of 904L ASS, the corrosion resistance of the passive film existed at the low Cl^- concentration is better than that existed at the high Cl^- concentration. The results of EIS are consistent with the results of potentiodynamic polarization.

Table 2. Interpreted values of resistance and capacitance for passive film.

$[Cl^-]$ (g/L)	R_f ($\Omega \cdot cm^2$)	CPE_f (F/cm^2)
20	4.404×10^5	2.052×10^{-5}
50	1.927×10^5	1.779×10^{-5}
78.5	5.054×10^4	2.540×10^{-5}
100	2.992×10^4	1.684×10^{-5}
120	1.986×10^4	2.253×10^{-5}

3.3 Current transient

Fig.4 shows the current transients of the 904L specimens in the BFG/water solutions containing the different Cl^- concentrations. In the cases of Cl^- concentrations for 20 g/L and 50 g/L, the current density is very low and no sudden increase with the extension of measured time, suggesting the occurrence of stable passivation. Further, in the case of Cl^- concentration for 78.5 g/L, the current density is also very low and no sudden in from 0 s to 700 s, but the current density increases suddenly when the measured time is up to 700 s. However, in the case of Cl^- concentration for 100 g/L, the presence of current fluctuation is observed, suggesting the occurrence of metastable pitting [20]. Finally, in the case of Cl^- concentration for 120 g/L, the current density increases with the extension of measured time, suggesting no occurrence of self-passivation. The above results of current transient are in agreement with the results of potentiodynamic polarization and EIS: the lower Cl^- concentration, the easier self-passivation.

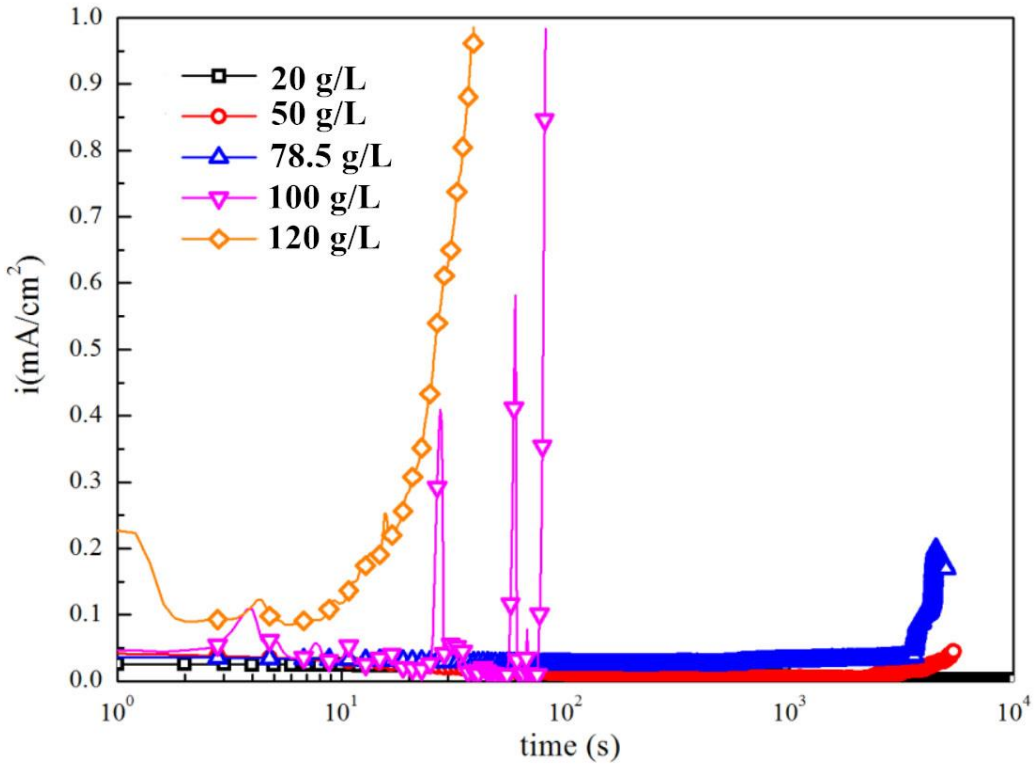

Figure 4. Current transients of 904L specimens in BFG/water solutions containing different Cl^- concentrations.

3.4Mott-Schottky plot

Fig. 5 shows the Mott-Schottky plots of the 904L specimens in the BFG/water solutions containing the different Cl^- concentrations. It is generally accepted that passive film on the surface of metals and alloys can be regarded as a semiconductor [28]. From Fig. 5, a positive value of slope on the straight line part for each Mott- Schottky plot is shown, indicating the passive film of 904L ASS is a n-type semiconductor. Based on Mott-Schottky equation for n-type semiconductors [29], the relationship between the space charge layer capacitance (C_{sp}) and the applied potential (E_{apply}) can be described as follows:

$$\frac{1}{C_{sp}^{\ 2}} = \frac{2(E_{apply} - U_{fb} - \frac{kT}{e})}{\varepsilon\varepsilon_0 e N_D} \quad (1)$$

In the above equation, U_{fb} is the flat band potential, k is the Boltzmann constant, T is the absolute temperature, e is the electron charge, ε is the dielectric constant of the passive film, $\varepsilon_0$is the permittivity of free space and N_D is the donor density.

In Equation (1), the two values of N_D and U_{fb} can reflect the corrosion electrochemical characteristics of metals and alloys. The value of N_D reflected the internal defects of passive film, and the N_D value would be interpreted by the slope of the straight line part on the Mott-Schottky plot [30]. Besides, the value of U_{fb} indicated the susceptibility of localized corrosion, and the U_{fb} value would be calculated by the extrapolation of the straight line part to 1/ $C_{sp}^{\ 2}$ = 0.

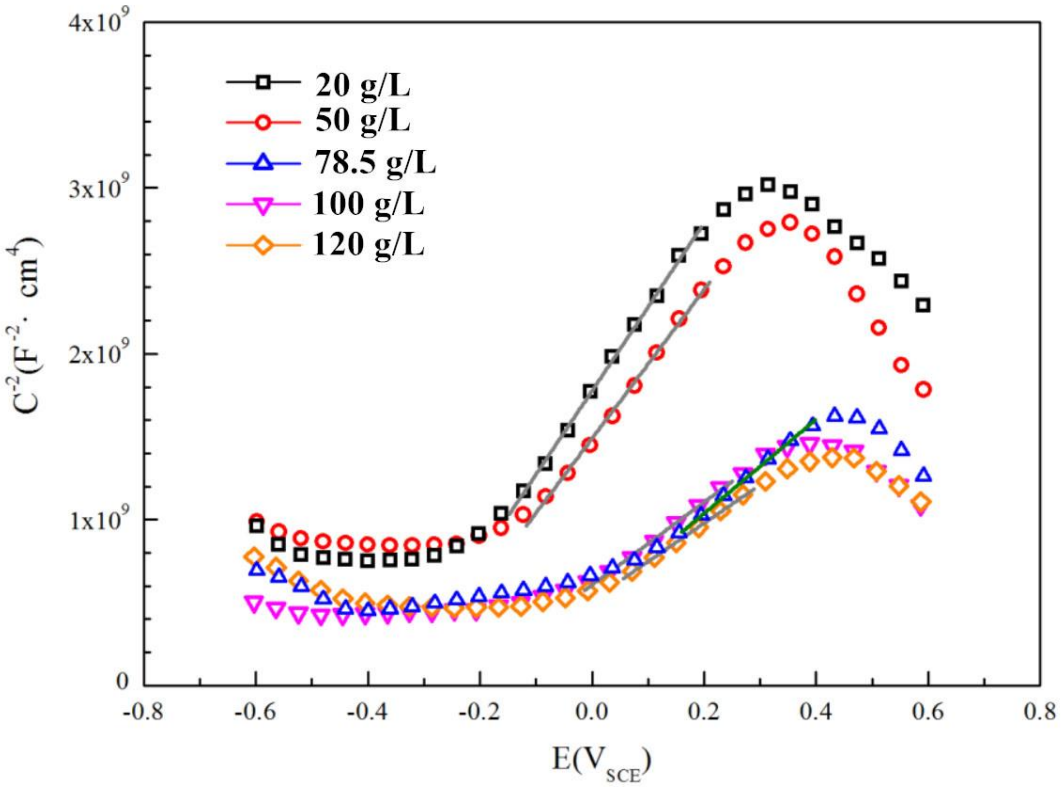

Figure 5. Mott-Schottky plots of 904L specimens in BFG/water solutions containing different Cl^- concentrations.

Table 3 shows the fitted values of N_D and U_{fb} from the Mott-Schottky plots, as shown in Fig. 5. The N_D values increase obviously with the increased Cl^- concentration, suggesting the internal defects of passive film at the low Cl^- concentration is less than that at the high Cl^- concentration. Besides, the U_{fb} values also confirm the influences of Cl^- concentrations on the corrosion electrochemical behavior of 904L ASS. The above results suggest that the self-passive characteristic of 904 steel decreases with the increased Cl^- concentration in the BFG/water system.

Table 3. Fitted values of donor density (N_D) and flat band potential (U_{fb}).

$[Cl^-]$ (g/L)	N_D (cm^{-3})	U_{fb} (V_{SCE})
20	1.968×10^{21}	-0.392
50	2.016×10^{21}	-0.332
78.5	3.199×10^{21}	-0.266
100	3.636×10^{21}	-0.243
120	3.919×10^{21}	-0.224

4. CONCLUSIONS

In this paper, influences of Cl^- concentrations on the corrosion electrochemical characteristics of 904L stainless steel in a simulated environmental solution that was acquired with the introduction of BFG into water were investigated by electrochemical techniques. The following conclusions were summarized:

(1) 904L stainless steel presented the electrochemical characteristic of self-passivation in the BFG/water solutions with the different Cl^- concentrations.

(2) The self-passive characteristic of 904L stainless steel was greater at the low Cl^- concentration than at the high Cl^- concentration.

(3) The influences of Cl^- concentrations on the corrosion electrochemical parameters of passivation current density, pitting potential, repassivation potential, passive film resistance and capacitance, donor density and flat bond potential was very significant.

References

1. B. Feng, Y.H. Kang, Y.H. Sun, Y. Yang and X.Z. Yan, *Int. J. Appl. Electromagn. Mech.*, 52 (2016) 357.
2. S.Y. Jiang, H.Q. Ding and J. Xu, *J. Tribol.-Trans. ASME*, 139 (2017) 014501-1.
3. X.T. Zheng, K.W. Wu, W. Wang, J.Y. Yu, J.M. Xu and L.W. Ma, *Nucl. Eng. Des.*, 314 (2017) 285.
4. J. Shi, J.F. Shi, H.X. Chen, Y.B. He, Q.J. Wang, Y. Zhang and G.Z. Li, *J. Press. Vessel Technol.-Trans. ASME*, DOI: 10.1115/1.4039344.
5. Y. Li, H. Ma, L. Cheng and D. Yu, *Electron. Lett.*, 54 (2018) 383.
6. Q.Y. Wu, J.Z. Dai and H.P. Zhu, *J. Earthqu. Eng.*, 22 (2018) 826.
7. Y.F. Kang, L.X. Fang, Y.H. Zhao and S.Y. Ren, *Math. Probl. Eng.*, DOI: 10.1155/2015/792069.
8. X.G. Feng, X.Y. Lu, Y. Zuo, N. Zhuang and D. Chen, *Corros. Sci.*, 103 (2016) 66.
9. H. Luo, H.Z. Su, C.F. Dong, K. Xiao, X.G. Li, *J. Alloy. Compd.*, 686 (2016) 216.

10. A. Alamr, D. F. Bahr and M. Jacroux,*Corros. Sci.*, 48 (2006) 925.
11. E.A.Abd El Meguid, N.A. Mahmoud and V.K. Gouda, *Birt. Corros. J.*32 (1996) 68.
12. V.S. Raja, S.K. Varshney, R. Raman and S.D. Kulkarni, *Corros. Sci.*, 40 (1998) 1609.
13. J. Michalska, B. Chmiela, J. Labanowski and W. Simka, *J. Mater. Eng. Perform.*, 23 (2014) 2760.
14. M.H. Moayed and R.C. Newman, Deteriroration in critical pitting temperature of 904L stainless steel by addition of sulfate ions, *Corros. Sci.*, 48 (2006) 3513.
15. X. Chen, Q.Y. Xiong, F. Zhu, H. Li, D. Liu, J.P. Xiong and Y. Zhou, *Int. J. Electrochem. Sci.*, 13 (2018) 1656.
16. Y. Zhou and F.A. Yan, *Int. J. Electrochem. Sci.*, 11 (2016) 3976.
17. G.C. Lv, C.C. Xu, Y.M. Lv, H.D. Cheng and Z.H. He, *Chin. J. Chem. Eng.*, 16 (2008) 646.
18. J. Tian and H.L. Huang, *Microelectron. Reliab.*, 78 (2017) 131.
19. Y.M. Tang, Y. Zuo, J.N. Wang, X.H. Zhao, B. Niu and B. Lin, *Corros. Sci.*, 80 (2014) 111.
20. X.G. Feng, X.Y. Lu, Y. Zuo, N. Zhuang and D. Chen, *Corros. Sci.*, 103 (2016) 223.
21. H.L. Huang, Z.Q. Pan, Y.B. Qiu and X.P. Guo, *Microelectron. Reliab.*, 53 (2013) 1149.
22. Y. Zhou, J.P. Xiong and F.A. Yan, *Surf. Coat. Tech.*, 328 (2017) 335.
23. Q.Y. Xiong, J.P. Xiong, Y. Zhou, F.A. Yan, *Int. J. Electrochem. Sci.*, 12 (2017) 4238.
24. Z.Y. Yong, J. Zhu, C. Qiu and Y.L. Liu, *Appl. Surf. Sci.*, 255 (2008) 1672.
25. Y. Zhou, H.J. Huang, P. Zhang, L. Dong and F.A. Yan, *Sur. Rev. Lett.*, DOI: 10.1142/S0218625X18502189.
26. F.G. Deng, L.S. Wang, Y. Zhou, X.H. Gong, X.P. Zhao, T. Hu and C.G. Wu, *RSC Adv.*, 7 (2017) 48876.
27. W.M. Jiang, Z.T. Fan, D.H. Liu and H.B. Wu, *Int. J. Adv. Manuf. Technol.*, 67 (2013) 2459.
28. Zhou, P. Zhang, Y. Zuo, D. Liu and F.A. Yan, *J. Braz. Chem. Soc.*, 28 (2017) 2490.
29. Y.F. Cheng and J.L. Luo, *Electrochimi. Acta*, 44 (1999) 2947.
30. Q.Y. Xiong, Y. Zhou and J.P. Xiong, *Int. J. Electrochem. Sci.*, 10 (2015) 8454